View metadata, citation and similar papers at core.ac.uk

brought to you by CORE

provided by IntechOpen

We are IntechOpen, the world's leading publisher of Open Access books Built by scientists, for scientists

4,800
Open access books available

122,000
International authors and editors

135M
Downloads

Our authors are among the

154
Countries delivered to

TOP 1%
most cited scientists

12.2%
Contributors from top 500 universities

CLARIVATE ANALYTICS BOOK CITATION INDEX INDEXED

WEB OF SCIENCE™

Selection of our books indexed in the Book Citation Index in Web of Science™ Core Collection (BKCI)

Interested in publishing with us?
Contact book.department@intechopen.com

Numbers displayed above are based on latest data collected.
For more information visit www.intechopen.com

22

Robot Manipulator Probabilistic Workspace Applied to Robotic Assistance

Fernando A. Auat Cheein, Fernando di Sciascio,
Juan Marcos Toibero and Ricardo Carelli
Instituto de Automatica, National University of San Juan
Argentina

1. Introduction

The probabilistic modelling of a robot manipulator workspace when combined with a Human-Machine Interface (HMI) allows the extraction and learning of the spatial preferences of the user. Furthermore, the knowledge of the most accessed zones of the robot's workspace permits the bounding of the time needed for the robot to reach a given position at its workspace.

From its early beginning, the use of robot manipulators within the robotic assistance field was concerned to emulate an orthopaedic arm (Fukuda et al, 2003; Zecca et al, 2002; Lopez et al, 2009). Therefore, the robot manipulator was considered as the final actuator of the assistive system where its main goal was to imitate the movements of an arm. Depending on the user/patient capabilities, the robot manipulator was commanded by either electro-myographic or electro-encephalic signals (Ferreira et al, 2006a; 2006b; 2008). A robotic device controlled by a Muscle-Computer Interface (MCI) can be found in (Artemiadis & Kyriakopoulos, 2006; Lopez et al, 2007; Millan et al, 2004; Ferreira et al, 2006b; Lopez et al, 2009; Ferreira et al, 2008). In these works, the electro-miographic signal is acquired, processed, classified and converted to motion commands. The system is closed by a bio-feedback loop. When used with a robot manipulator, a MCI is usually connected to a set of muscles that the patient is able to move at its own will. The number of channels used by the interface increases as increases the number of the degrees of freedom (DOF) of the robot (Yatsenko et al, 2007; Lopez et al, 2009; Ferreira et al, 2008). Thus, for a single 2DOF robot manipulator are necessary three different muscles: two to govern each DOF and a third to set a sign (if the manipulator is moving to the left or to the right), for a direct control of the robot manipulator.

For robotic devices controlled by Brain-Computer Interfaces (BCI's), the situation is analogous to the MCI; the number of signals or patterns to be extracted from the EEG (electro-encephalogram) increases as increases with the number of DOF's –or actions– to be performed by the robot. Although most applications of BCI's are oriented to govern a mobile robot –because of its direct analogy with a motorized wheelchair (Bastos Filho et al, 2007a; Bastos Filho, 2007; Ferreira et al, 2008; Bastos Filho et al, 2007b)– some works have been published showing the implementation of a BCI to control the movements of a robot

manipulator (Oskoei & Hu, 2007; Farry et al, 1996; Auat Cheein et al, 2007a; Auat Cheein et al, 2007b; Auat Cheein et al, 2008).
The way that the patient interacts with the interface is determined by the objective of the HMI. Thus, for a HMI connected to a robot, the proper motion of the automata serves as a bio-feedback channel to the user (Wolpaw et al, 2002 ; Ferreira et al, 2008). A more suitable way to interact with the user is by means of scan modes. The scan modes have been widely used in the recent years for assistance technology. It is not restricted only to BCI's or MCI's but to most of HMI.
The scan mode applied to a HMI's in robotic assistance is mainly composed by a series of icons; each icon represents an action or a place attached to the robotic task; the patient, using its biological signals, displace the scan over the several icons; once an icon is selected –also using the biological signals– the robot performs the task associated with the selected icon. This kind of interface decreases the effort of the user when generating the biological signals, relegating the control of the interface to the control of the scan. Moreover, some HMI include an automatic scan; thus the user only has to accept –or cancel if needed– an icon within the scan. Figure 1 shows a general architecture of a HMI with a scan mode incorporated.

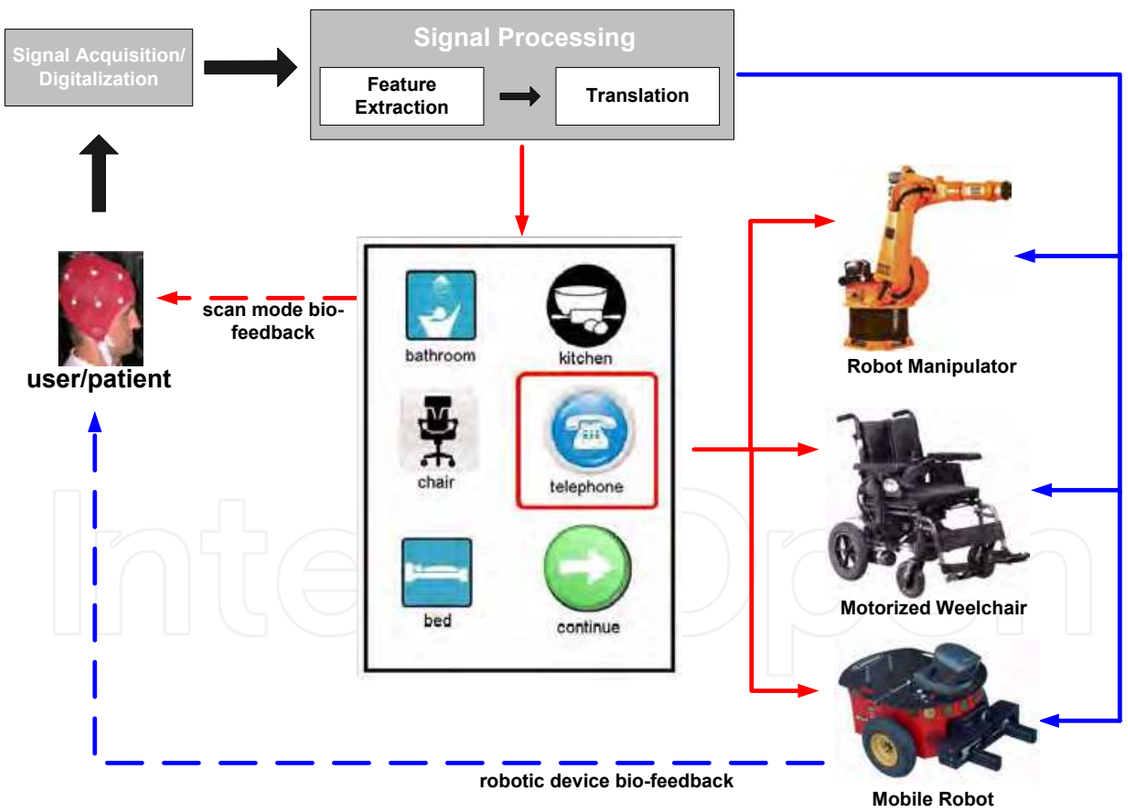

Fig. 1. General architecture of a HMI. The dashed and solid blue-lines correspond to a HMI that control the robotic device in a direct way; the solid and dashed-red lines refer to a HMI with a scan mode incorporated on it.

Figure 1 shows the general architecture of a HMI. When the HMI has a scan mode, the bio-feedback loop is closed by both the robot's movements and the scan mode itself. As was stated before, the scan mode reduces the work of the HMI's user, although it restricts the interface to a number of actions associated with the icons within the scan.
In this work we show the implementation of a robot manipulator workspace scan mode applied to a HMI. Although we have used a BCI, any other HMI can be adapted to the system presented in this work. The robotic device used is a SCARA robot manipulator (Sciavicco & Siciliano, 2000). The robot's workspace is divided into cells. Each cell has a probability value associated with it. The scan mode is run according the probability information of the cell, decreasing in that way the time needed for the robot to reach the desire cell. Once a cell is chosen by the user, the robot manipulator reaches the center of mass of the cell using a kinematic controller.
Three types of scan modes are shown in this work: an uniform scan mode and two based on the probabilistic information of the workspace. The three scan modes are tested by Monte Carlo experiments. The probability-based scan modes learn the preferences of the patient by the measure of the probability of a cell in being selected by the user. The probability value of each cell at the robot's workspace is dynamically maintained according to the patient cell's selection. Considering that the robot's workspace behaves as a probability density function, the Kullback-Liebler (relative entropy) measure is shown in order to establish a measure of divergence between the different scan modes.

2. Overview of the System

The main objective of the HMI is that the user/patient be capable of generating a set of commands by means of his/her biological signals in order to control the robotic device used. In this work, the HMI used is a BCI but is not restricted to it. The BCI is controlled by event related potentials (ERP) acquired from the occipital lobe of the patient. Such potentials are the event related synchronization/desynchronization (ERS/ERD). The ERS/ERD potentials are measured in the alpha band (8–13 Hz) of the EEG from the occipital lobe. The BCI conform an alphabet of commands from the ERS and ERD which are then sent to a Finite State Machine (FSM). The FSM contains actions or desired behaviors of the robot to be performed if the user generates the appropriate command. The BCI was tested in a population of 25 cognitive normal volunteers and the results can be seen in (Ferreira et al, 2008).
The robot manipulator is the actuator device that completes the HMI system. The robot used in this work is a SCARA type, Bosch SR-800 (see Fig. 2). In the absence of perturbations and without considering gravity effects, the dynamic of a rigid robot manipulator with n joints can be expressed as (1).

$$M(q)\ddot{q} + C(q,\dot{q})\dot{q} + f(\dot{q}) = \tau \tag{1}$$

In (1), q is an $n\times1$-array of joint angular positions; τ is an $n\times1$-array of applied torques; $M(q)$ is the $n\times n$ positive definite inertia matrix; $C(q,\dot{q})$ is an $n\times n$ matrix of centripetal and *Coriolis* effect and $f(\dot{q})$ is an $n\times1$-array of friction moments. More information about the robot's parameters can be found in (Bastos Filho et al, 2006 ; Ferreira et al, 2006c).

Considering that the objective of the HMI is to position the robot manipulator at a specific cell of its workspace, a kinematic controller was used (Kelly et al, 2004).

Fig. 2. Robot manipulator Bosch SR-800.

3. Sequential Scan Mode

The scan mode developed in this work is an automatic one. The workspace of the robot manipulator is divided into cells. As a first approach lets considerer that the cells do not have a probability value associated with them. Thus, the probability of a cell to be chosen by the patient is the same for all the cells at the robot's workspace. Moreover, the probability of being scanned is also the same. Figure 3.a shows the cells' distribution of the robot's workspace. The number of cells can be increased if the application requires it. Instead of scanning cell by cell, the robot's workspace is divided into three main zones. Then, the scan mode is first made zone by zone until one zone is selected by the user (see Fig. 3.b). Once a zone is selected, the scan is made row by row of the selected zone. If after three row-by-row scans, no row is selected, the scan returns to be executed zone-by-zone. On the other hand, if a row is selected, then the scan passes to be cell-by-cell until a cell is selected (see Fig. 3.c). The scan returns to be row-by-row if no cell is selected after three runs. Once a cell is selected, the robot is positioned at the center of mass of the cell and the scan mode begins again zone-by-zone.

The three zones division of the robot manipulator's workspace is based on the fact that a normal limbed patient grasps the elements of the environment from the right, center or left to his/her body.

The final interface is presented in Fig. 4.

a)

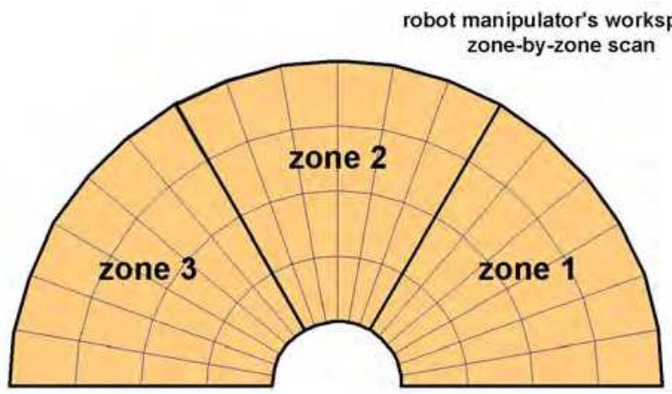

b)

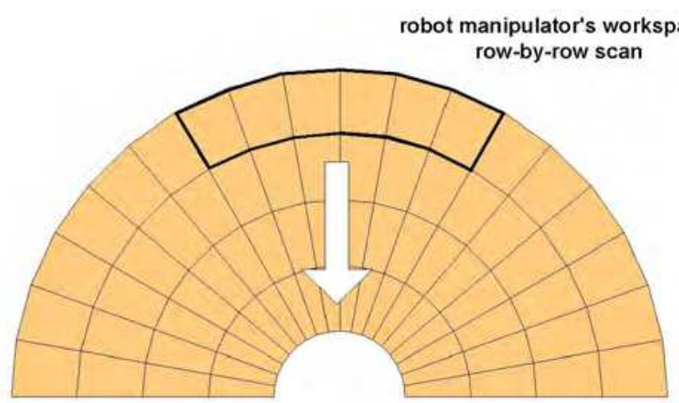

c)

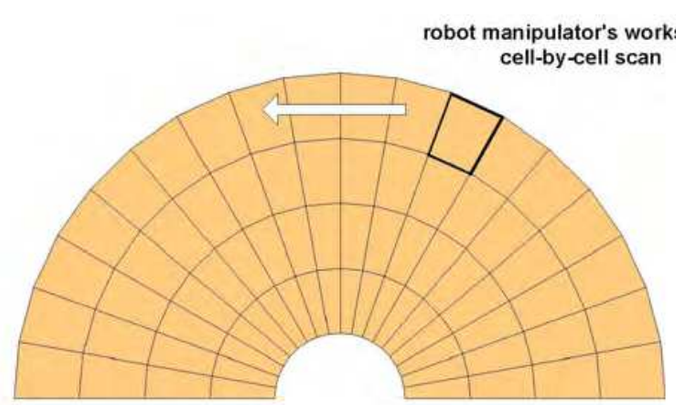

Fig. 3. Sequential scan mode. a) The scan is first executed zone-by-zone until one zone is selected by the user; b) then the scan is executed row-by-row of the selected zone; c) the scan is run cell-by-cell of the selected row.

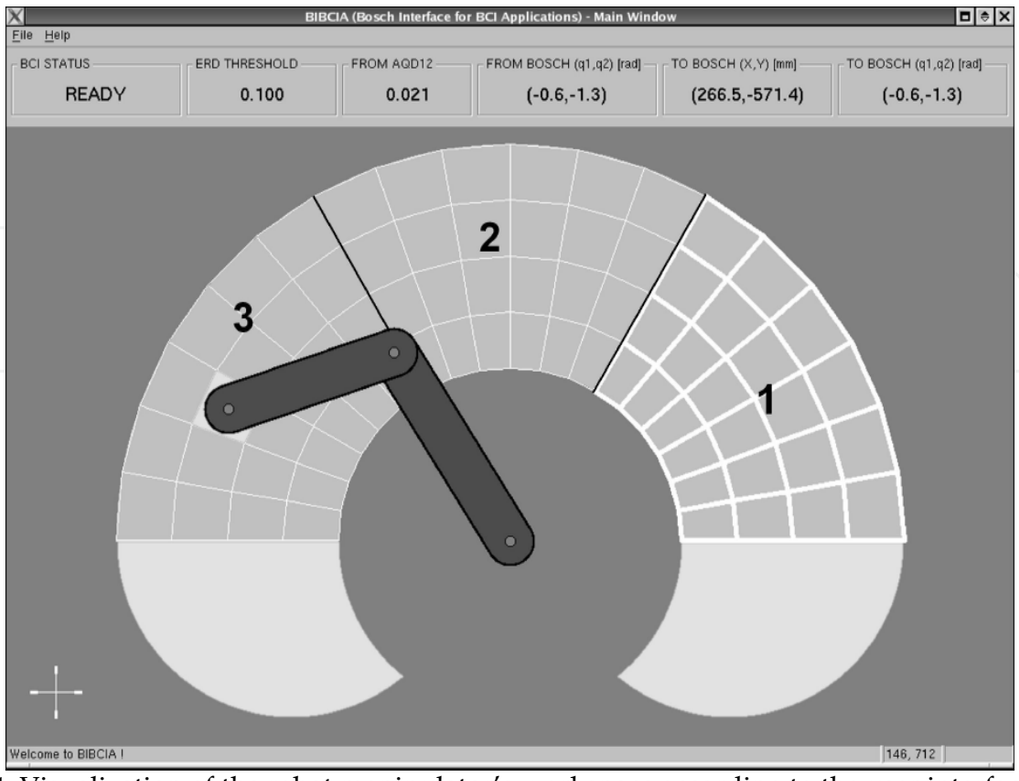

Fig. 4. Visualization of the robot manipulator's workspace according to the user interface.

4. Probability-based Scan Mode

Two probability-based scan modes have been implemented in this work. A first approach is based on maintaining the workspace zones with a fixed number of cells. On the other hand, the second approach has a variable number of cells assigned to each zone depending on their probability values. The probability value in both approaches represents the probability of accessing a cell.

4.1 First Approach: Fixed zones division

The first approach of the probability-based scan mode works as follows:

- The workspace resolution is set to 72 cells (4 rows and 18 columns) and can be easely changed depending on the application. The worspace behaves as a *pmd* (probability mass distribution) and can be interpreted as a *4×18*-matrix (where $c_{i,j}$ is the cell at the *i*-row and *j*-column).
- When the HMI is loaded by the first time, the robot's workspace has a uniform distribution over their cells ($p(c_{i,j}) = 1/72$, con $i = 1..4$ and $j = 1..18$).
- Each zone (see Fig. 4) has a probability value associated with it, which is the sum of the probability values contained in each zone. Thus, for example:

$p(zone_1) = \sum_{i=1,j=1}^{i=4,j=6} p(c_{i,j})$. Also, each row's probability equals the sum of the probability value of the cells contained in that row. This is so because the robot's workspace is considered as a *pmd*, then the sum of all probability values of the cells sum the unity.

- The division of the zones remain unchanged with the evolution of the probability values of the cells.
- The scan starts at the zone with the highest probability value. If such a zone does not exists, the scan starts at the rightest zone (i.e., zone 1 in Fig. 4). The scan highlights one zone at a time and waits 2 seconds (Ferreira et al, 2008) until passing to the next zone. The scan is cyclic, which means that if the scan has passed from zone 2 to zone 3, it then goes to zone 1 instead of returning to zone 2.
- Once the patient selects a zone –using his/her ERS/ERD potentials– the scan is made row-by-row in the selected zone. As before, the scan starts at the row with the highest probability value and runs decreasing to the row with the lowest probability value of the same zone. The scan is also cyclic. Once a row is selected, the scan is run cell-by-cell of the selected row only, starting from the cell with the highest probability value.
- Once a cell is selected, the robot manipulator is driven to the center of mass of such a cell and the probability value of it is updated. The update procedure is performed by the recursive *Bayes* rule. Once a probablity value of a cell is updated, the probability values of all cells at the robot's workspace are also updated. The update procedure is shown in the following sections.
- When the scan is on the row-by-row mode or cell-by-cell mode, after three runs with no selection, the scan returns to its previous mode.
- Finally, in every mode, the scan waits 2 seconds before changing the highlighting.

4.2 Second Approach: Dynamic zone division

The second approach works under the same criteria of the first approach: the workspace is divided into three zones, although in this case, the number of cells that belong to each zone is determined by their probability values. The scan mode can be summarized as follows.

- When the scan starts the first time, the robot's workspace is considered as a uniform probability mass distribution; each cell has the same probability value. The scan mode up to this point has the same execution than the first approach. Experimentally was determined that after 20 runs (i.e., twenty cells were reached by the robot manipulator) the dynamic zone's division is able to be performed.
- Let a and b be the higher and lower probability cells' values respectively after the first 20 runs. Then, the workspace is divided into three zones according to these values. Table 1 shows how the division is made. The number of cells belonging to each zone is now governed by their probability values and is not a fixed number –of 24 cells– as it is in the first approach.
- Then, each zone is divided into three sub-zones under the same criteria of the last paragraph: each one of these sub-zones contains a set of probability weighted cells according to Table 1 but divided with respect to the zone instead the workspace.

- The scan mode proceeds as follows:
  - First, the zone with the highest probability value at the workspace is highlighted. If after two seconds this zone is not selected by the user of the HMI, the second probability zone is highlighted. If it is not selected, the highlight passes to the third and last zone –which has the lowest probability value associated with it–. The scan is cyclic –as it is the first approach– and the probability of each zone equals the sum of the probability values of the cells contained within them.
  - When a zone is selected, the scan highlights the sub-zone with the highest probability value inside the previous zone. Thus, all cells within this sub-zone are highlighted. Also, the cells may not be consecutive. If the user does not select this sub-zone, the scan passes to the next one. The scan mode is also cyclic.
  - Once a sub-zone is selected, the scan highlights each cell of the current sub-zone. In this case, the scan starts at the cell with the highest probability value associated with it and finishes at the cell with the lowest probability value. If all cells of the sub-zone have the same probability value, the scan starts randomly.
  - At every stage, the scan is cyclic and remains highlighting during two seconds before changing. If no selection is performed by the user after three runs, the system returns to the previous scan mode.
  - If a cell is selected, the probability value of the cell and of the rest of the cells of the workspace is updated according to the recursive *Bayes* rule.
  - The dimensions of the zones and sub-zones are re-calculated after a cell is selected.

a_t	Highest probability cell value at time t
b_t	Lowest probability cell value at time t
$zone1 = \left\{ \forall c_{i,j}, i = 1..4, j = 1..18 : b_t + \frac{2}{3}(a_t - b_t) < p(c_{i,j} \mid W) \le a_t \right\}$	Zone 1: is the set of all cells whose probabilities are the highest of the workspace (W)
$zone2 = \left\{ \forall c_{i,j}, i = 1..4, j = 1..18 : b_t + \frac{(a_t - b_t)}{3} < p(c_{i,j} \mid W) \le b_t + \frac{2}{3}(a_t - b_t) \right\}$	Zone 2: is the set of all cells whose probabilities are of middle range
$zone3 = \left\{ \forall c_{i,j}, i = 1..4, j = 1..18 : b_t \le p(c_{i,j} \mid W) \le b_t + \frac{(a_t - b_t)}{3} \right\}$	Zone 3: is the set of all cells with the lowest probability values.

Table 1. Workspace zones definitions.

As it can be seen, the number of cells that belong to a sub-zone or zone is variable. Then, the organization of the zones at the robot's workspace is dynamic. This allows the improving of the scan mode in order to access in a priority way to the most probably cells.

4.3 Recursive *Bayes* Rule

The probability update of each cell at the robot's workspace is based on the recursive *Bayes* rule (Fishman, 1996 ; Papoulis, 1980). Once the patient directs the HMI to access a specific cell, the probability value of that cell changes according to (2).
Let $c_{i,j}$ be a cell at the robot's workspace and G a zone to which that cell belongs (e.g., *zone 1*). Thus, the updating algorithm is given by,

$$p_t(c_{i,j}\,|\,G) = \frac{p_t(G\,|\,c_{i,j})\,p_{t-1}(c_{i,j}\,|\,G)}{p_t(G\,|\,c_{i,j})\,p_{t-1}(c_{i,j}\,|\,G) + p_t(G\,|\,\bar{c}_{i,j})\,p_{t-1}(\bar{c}_{i,j}\,|\,G)} \tag{2}$$

In (2), $p_t(c_{i,j}\,|\,G)$ is the current probability of the cell $c_{i,j}$ given the zone G; $p_{t-1}(c_{i,j}\,|\,G)$ is the previous probability value of $c_{i,j}$. Though (2) is mainly used in very simple applications (Auat Cheein et al, 2008; Ferreira et al, 2006c) it fits as an updating rule for the purpose of this work. The rest of the cells at the robot's workspace are also updated using (2), but with $p_t(\bar{c}_{i,j}\,|\,G)$ -the probability of $c_{i,j}$ not been selected with respect to the zone- instead of $p_t(c_{i,j}\,|\,G)$ in the appropriate places of (2).

In order to make sense to the use of the recursive *Bayes* rule, an initial probability value must be given to all cells at the workspace. Thus, it is initialized as a uniform *pmd*. Figure 4 shows the evolution of a cell's probability when it is successively accessed by the patient. As the probability of this cell tends to 1, the probability value of the non-accessed cells tends to zero according to (2).

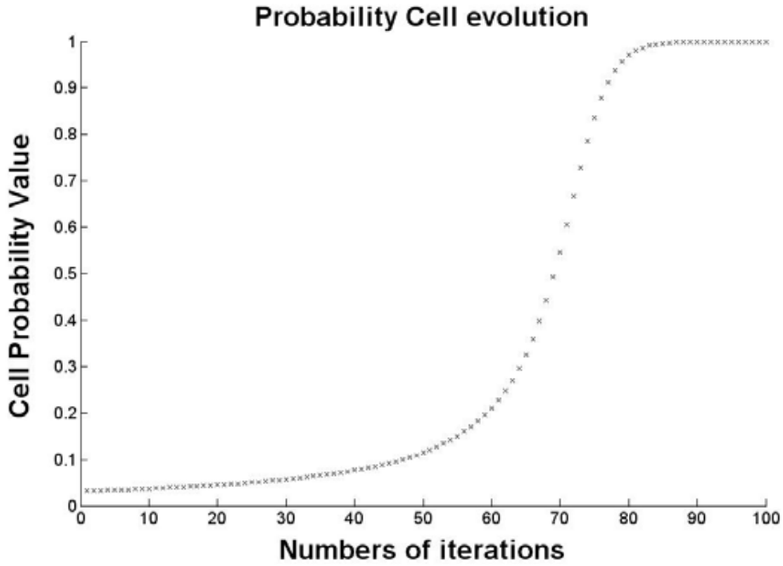

Fig. 4. Probability cell evolution when it is constantly accessed (Auat Cheein et al, 2008).

Considering that the scan mode of this approach is based on the probability weight of the cells of the robot's workspace, if a cell, e.g., has the highest probability value of the *zone 2* at time t, and it is successively accessed, then at the instant $t + k$ that cell might abandon the

zone 2 -because of it probability value increases- and enter to *zone 1*. Nevertheless, having into account that zone 1 is composed by those cells with the highest probability values of the entire robot's workspace, then the cell that has recently enter this zone, might not be one of the first to be scanned. This situation will be shown in the experimental results.

5. Experimental Results

This section shows the time consuming differences of the three scan modes shown in this work. In order to do this, a Monte Carlo experiment was designed (Auat Cheein et al, 2008; Fishman, 1996). The time analysis establishes a performance comparison between the three scan modes. In addition, the final distribution of the robot's workspace for a right-handed user after 100 trials is also shown. This distribution is shown for both probability scan modes –the accessed cells are the same–. The Kullback-Liebler relative entropy is calculated between both probability-based workspaces in order to establish a divergence value.

5.1 Monte Carlo Experiment

In this work, the robot's workspace is divided into 72 cells (see Fig. 3). It also can be considered as a *4×18-matrix*. Then, a cell's position can be defined by the number of row and column of the *4×18-matrix*. Considering the number of row and column as a random variable, the Monte Carlo experiment was designed as follows:

- A uniform random source generates two random variables: x and y.
- The random variable x is mapped into the rows of the robot's workspace (m).
- The random variable y is mapped into the columns of the robot's workspace (n).
- The pair <m,n> determines the position of a cell at the robot's workspace. This cell is the one that will be accessed by the scan modes. The three scan modes start.
- The time needed by the patient to reach a cell is recorded for each scan mode.
- Once the robot reaches the proposed cell, a new cell is generated and the process starts all over.

5.2 Mapping Functions

Let f_x be a row mapping function of the form,

$$\begin{aligned} f_x &: A \to B \\ x &\to m \end{aligned} \tag{3}$$

where $A = \{x \sim U(0,1)\}$ and $B = \{m : m \in \{1,2,3,4\} \subset N\}$, with N the set of positive integers. Let also f_y be a column mapping function of the form,

$$\begin{aligned} f_y &: A \to C \\ y &\to n \end{aligned} \tag{4}$$

where A is again $A = \{x \sim U(0,1)\}$ and $C = \{n : n \in \{1,2,...,18\} \subset N\}$. Equations (3) and (4) show the domain and range of the mapping functions. The mapping is made according to the following statements (Auat Cheein et al, 2008).

- Let $p(c_{i,j})$ the probability value of a cell located at the *i-row* and *j-column* of the robot's workspace.
- Let x be an outcome of the uniform random source f_x.
  - If $0 \le x \le \sum_{i=1, j \in C} p(c_{i,j})$, then $f_x(x) = i = 1$. This means that the value of $x \in A$ should be lower than the sum of all probability cell's values over row 1 for $f_x(x)$ be equal to 1.
  - If $\sum_{i=1, j \in C} p(c_{i,j}) \le x < \sum_{i=2, j \in C} p(c_{i,j})$, then $f_x(x) = i = 2$. This means that $x \in A$ should be greater or equal to the sum of all probability cell's values over row 1 and lower than the sum of all probability cell's values over row 2 for $f_x(x) = i = 2$.
  - The process continues up to the last row whose expression is: if $\sum_{i=3, j \in C} p(c_{i,j}) \le x \le \sum_{i=4, j \in C} p(c_{i,j})$, then $f_x(x) = i = 4$.
- For the mapping over rows, the procedure is the same. However, in this case, the sum of probability values is made over the columns.
- Each time a cell is reached by the scan, the mapping functions (f_x and f_y) vary. It is so because these functions depend on the probability values of the cells at the robot's workspace. Thus, the most accessed cells will have more probability in being mapped. This allows us to emulate, e.g., a right-handed user.

5.3 Monte Carlo Simulation Results

The objective of the Monte Carlo experiments was to test the performance of both scanning methods: probability-based and sequential ones. The performance is measured in function of the time needed to access a given position. This position is generated by the uniform random source shown in (3) and (4). After 500 trials the mean time needed to access a random position by the first approach of the probability-based scan was of 16.8 seconds. For the second approach of the probability-based scan the mean time needed was of 20.4 and for the sequential scan was of 19.8 seconds. The three results are in the same order but the probability based first approach of the scan mode requires less time.

Lets consider now only the right side of the workspace. This situation is suitable for a right-arm amputee patient. The mean time of access for all points belonging to the workspace right side is of 8.4 seconds under the second approach of the probability-based scan instead of 11.3 seconds corresponding to the first approach of the probability-based scan mode. Under sequential scan, the mean time is of 14.8 seconds. The probability-based scan mode second approach is 43% faster than the sequential scan for cells over the right side of the workspace whereas the first probability-based approach is 23.7% faster. Details of these results can be seen in (Auat Cheein et al, 2008). The accessing time values can be interpreted as the patient needs an overall time of 8.4 seconds to access any cell of the right side of the robot's workspace using the second scan mode approach instead of 11.3 seconds of the first

probability-based approach. If the whole workspace is to be used, then the first approach is more convenient.
The Figures 5 and 6 show the mapping function for the probability-based scans at the end of the Monte Carlo simulation. The mapping functions are dependent on the probability values of the cells.

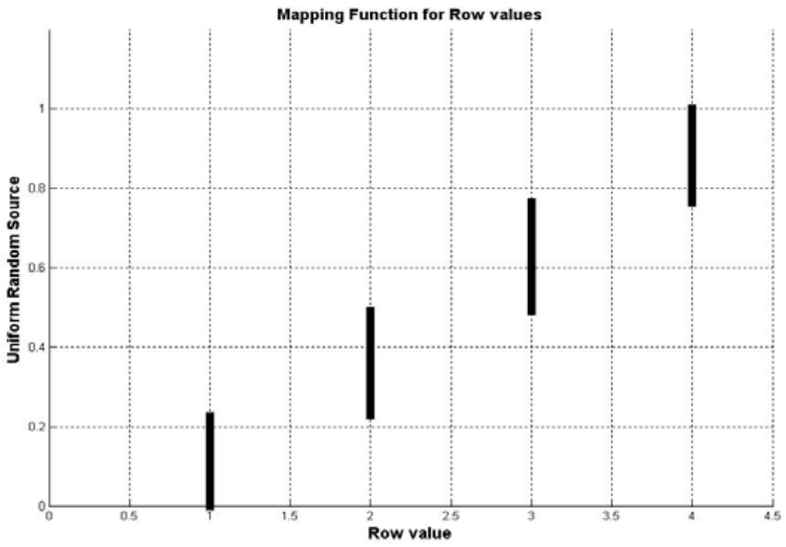

Fig. 5. Row mapping function of the Monte Carlo experiment –see Eq. (3)–.

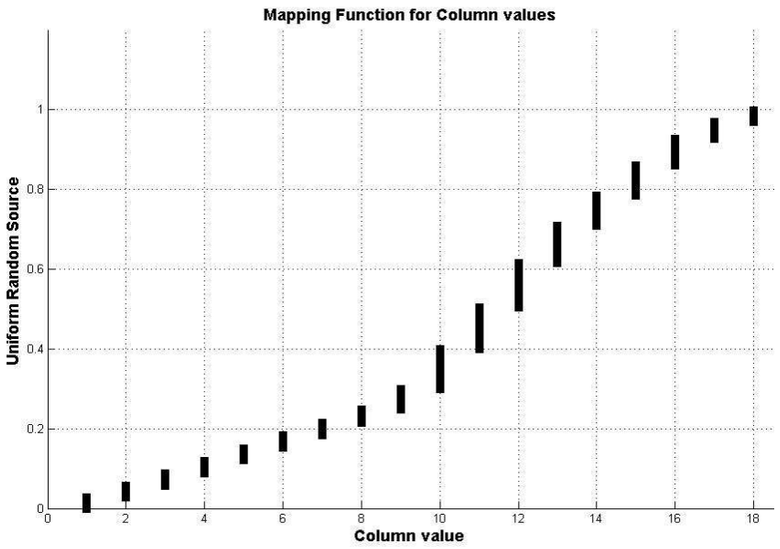

Fig. 6. Column mapping function of the Monte Carlo experiment –see Eq. (4)–.

In *section 4.3* was stated that a cell may change of zones as its probability grows or decrease during the scan mode of the second probability-based approach. Figure 7 shows this situation. A specific cell was successively accessed (see Fig. 4). The cell was initially in *zone 3*

(the group with the lowest probability value). During the successive calls of the cell, its probability was growing and the cell passed from *zone 3* to *zone 2* and then to *zone 1*.

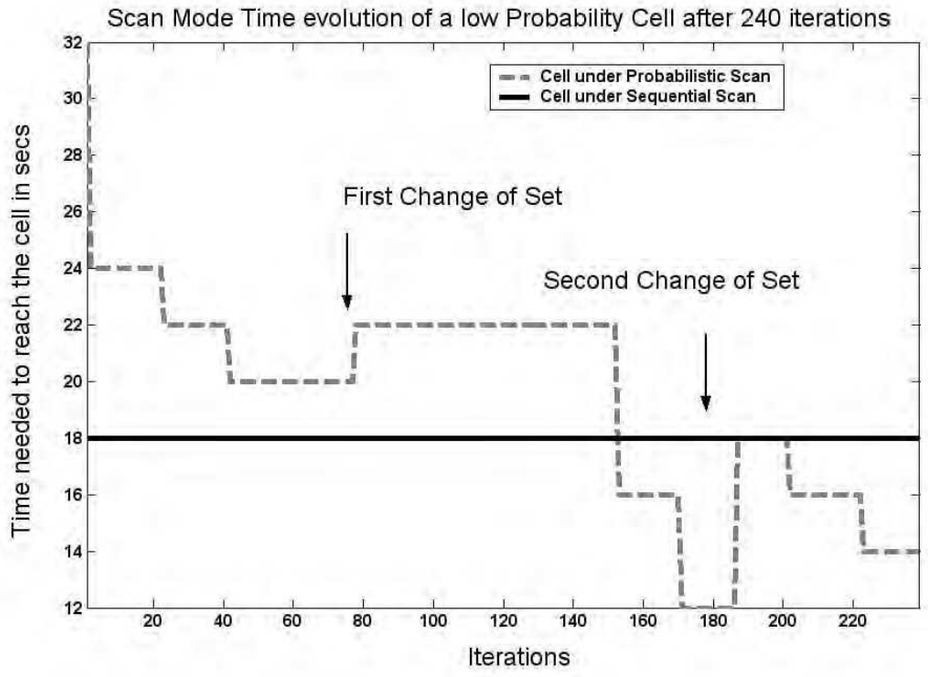

Fig. 7. Evolution of the accessing time of a cell during successive calls.

Figure 7 shows that the time of access of the cell by the sequential scan mode remains constant whereas varies for the second approach of the probability-based scan mode. When a cell changes to a greater probability zone, it abandons its scan priority. Thus, if it was previously in *zone 3* with the highest probability value in that zone (it is the first cell in being scanned inside that zone), when it passes to *zone 2* it will be one of the cells with the lowest probability value of that zone. This situation explains why the time of access of a cell grows every time a cell change its zone (as it is shown in Fig. 7). Nevertheless, the final time of access is lower than the initial value.

Figure 8 shows the final zone's division of the robot's workspace at the end of the Monte Carlo experiment for the two probability scan mode approaches. Figure 8.a shows the probability workspace distribution for the first probability based scan mode approach; the *zone 2* represents the most accessed zone. This situation means that, for a right-handed user, every location at the front of the hand will be the most reached. Figure 8.b shows the probability workspace distribution of the second probabilistic scan mode approach. The *zone 3* -which contains the cells with the lowest probability according to Table 1- is limited by a solid-black line; *zone 2* is formed by those cells with a solid-blue line at their limits. The *zone 1* -the set of cells with the highest probability value according to Table 1- remains unbounded in Fig. 8.b. The probability value of the cells and zones in Fig. 8 is represented by the gray-bar at the top of each figure.

a)

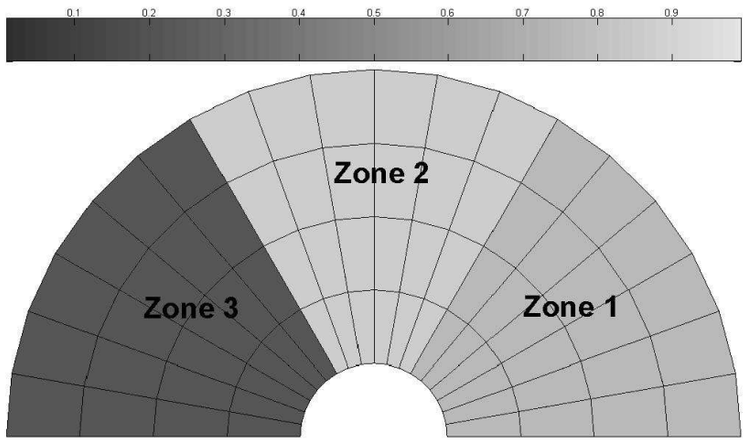

b)

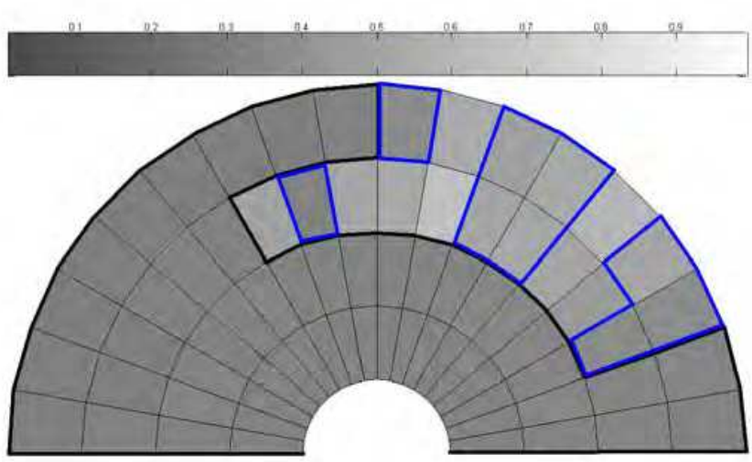

Fig. 8. Robot's workspace zones' division after the Monte Carlo experiment. a) Zones probability distribution according to the first approach of the probability scan mode. b) Cells probability distribution according to the second approach of the probability-based scan mode; cells with the lowest probability value -*zone 1*- are limited by the solid-black line; cells of the zone 2 are bounded by a solid-blue line; cells of the *zone 1* -with the highest probability value- remain unbounded.

5.4 Right-handed Workspace Distribution

Figure 8 has shown the zones divisions for the two probability-based scan modes for the Monte Carlo experiment. Figure 9, on the other hand, shows a real workspace distribution for a right-handed user. For the experiment, the BCI connected to the HMI was used. Figure 9 shows the cell's probabilities after 100 trials. As it can be seen, the right side of the workspace is the most accessed one.

By inspection, it is possible to see that both workspaces' *pmds* shown in Fig. 8 look very

similar. Considering that the *pmd* represents the learning of the HMI with respect to the patient's needs, the Kullback-Liebler relative entropy is calculated between both *pmds* of Fig. 9 in order to have a divergence value of the workspaces probability mass distributions.

a)

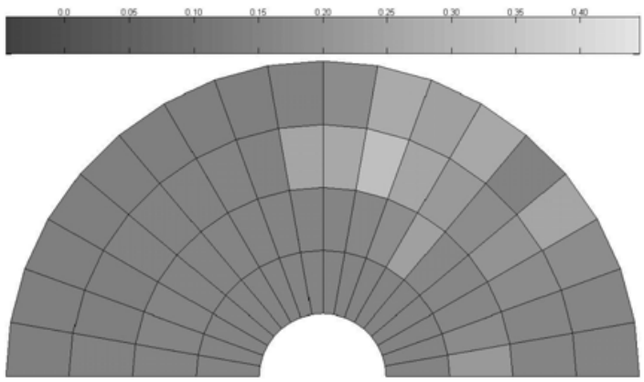

b)

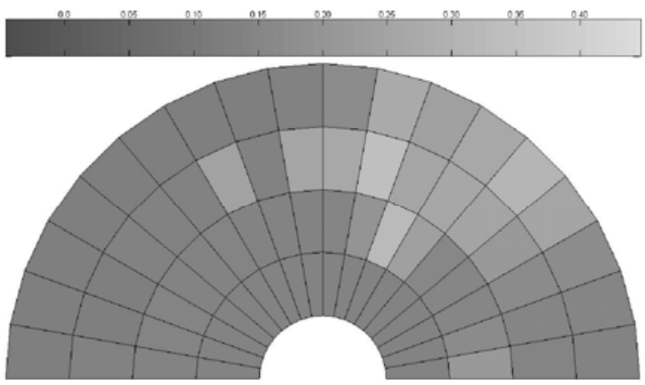

Fig. 9. Cells probability values for the two probability scan modes approaches after 100 trials. a) Final workspace's *pmd* for the first approach of the probability-based scan mode. b) Final workspace's *pmd* for the second approach of the probability-based scan mode. The difference between both *pmds* lies on the fact that the recursive *Bayes* rule is calculated based on the zone's probability information and not the workspace's probability (which is the unity).

5.5 Kullback-Liebler divergence

The Kullback-Liebler relative entropy is a pseudometric (Cover & Thomas, 2006) that gives a measure of the divergence between two probability density functions and it is presented in (5) -for the continuum case- and (6) -for the discrete case-. The reference functions in (5) and (6) are $g(.)$ -density function- and $q(.)$ -mass function- respectively.

$$D_{f||g} = \int_{-\infty}^{\infty} f(x)\log(\frac{f(x)}{g(x)})dx \tag{5}$$

$$D_{p||q} = \sum_{x=-\infty}^{\infty} p(x)\log(\frac{p(x)}{q(x)}) \tag{6}$$

Considering that the set of cells is the same for both probability based scan modes approaches, equation (6) is directly applied to the *pmds* of the robot manipulator. Thus, for the experiment shown in Fig. 9, the divergence between the first workspace probability based scan mode approach and the second workspace probability-based scan mode approach is of 0.0832. Thus, it is possible to say that both probability scan modes approaches lead to a very similar workspace's *pmds* -both learn the user's preferences in the same way-.

6. Conclusion

This work has shown the implementation of three scan modes of a robot manipulator workspace governed by a Human Machine Interface. The first scan approach was a sequential one with no consideration of preferences of the user/patient of the HMI. The other two scan approaches were based on the probability information attached to every cell at the robot's workspace. The probability value was updated by means of the recursive *Bayes* rule. The whole workspace was seen as a single probability mass distribution. Thus, each cell's probability value reflects the times that cell was accessed by the user and it governs the scan (the probability of been accessed). The cells with the highest probability value will be scanned first.

A time analysis between the three methods presented here showed that the probability-based scans improves the access time of the most accessed cells. Thus, if the HMI is going to be used for the first time (the robot manipulator workspace is an uniform *pmd*), the first approach of the probability-based scan mode has shown a better performance than the other approaches. On the other hand, once the preference of the patient (right/center/left side of the workspace) is well defined, the second approach of the probability based scan mode has shown lesser time requirements.

Although the system was primary designed to be implemented via a Brain Computer Interface, it could be used with any HMI with the same Finite State Machine implemented on it.

Experimental results showed that the time needed to access a specific position at the workspace is decreased each time that position is reached. This is due to the fact that the recursive *Bayes* algorithm implemented updates the probability value of the selected position after it is reached by the robot. A decrement of the time of access implies less effort by the user/patient of the HMI in reaching the objective.

In this work, a right-handed workspace distribution case was presented. This case showed that all cells to the right of the workspace have the higher probability value and the lower time needed to be accessed.

The robot workspace resolution was set to 72 cells in this work, although it could be adjusted according to the HMI destination. In addition, the interface can be extended to operate in 3D.

The probabilistic workspace configuration learns the user's preferences and uses this knowledge in the scan mode. It pays special attention to those cells with the highest probability value thus minimizing the time needed to access them.

7. References

Artemiadis, P.K. & Kyriakopoulos, K.J. (2006). EMG-based teleoperation of a robot arm in planar catching movements using ARMAX model and trajectory monitoring techniques. *IEEE Int. Conf. on Robotics and Automation*, pp. 3244-3249, ISBN: 0-7803-9505-0, Orlando, US, may 2006.

Auat Cheein, F.; di Sciasio, F.A.; Bastos Filho, T. & Carelli, R. (2007a). Probabilistic Scan Mode of a Robot Manipulator Workspace using EEG signals. *Journal of Physics: Conference Series*, Vol. 90, ISSN 1742-6588.

Auat Cheein, F.; di Sciasio, F.A.; Bastos Filho, T. & Carelli, R. (2008). Towards a Probabilistic Manipulator Robot´s Workspace Governed by a BCI. In: A. Fred, J. Filipe, and H. Gamboa (Eds.): *BIOSTEC 2008, CCIS 25. (Org.). Communications in Computer and Information Science.* Berlim: Springer-Verlag, 2008, 1, p. 73-84. ISBN: 1865-0929.

Auat Cheein, F.; Ferreira, A.; Bastos Filho, T.; di Sciasio, F.A. & Carelli, R. (2007b). Probabilistic Scan Mode of a Robot Manipulator Workspace using EEG signals. Part II. *Journal of Physics: Conference Series*, Vol. 90, ISSN 1742-6588.

Bastos Filho, T.F. (2007). Equipment Design and Development Directed for Human Rehabilitation. *Workshop on Robotics Applications and Automatic Control ROBCON'07*, 1, 1-78, ISSN:

Bastos Filho, T.F.; Ferreira, A.; Celeste, W.C.; Auat Cheeín, F. & Sarcinelli Filho, M. (2006). Human-Machine Interfaces Based on EMG and EEG Applied to Robotic Systems. *Proc. of the 2nd Int. Workshop on Biosignal Processing and Classification - Biosignals and Sensing for Human Computer Interface / ICINCO (Int. Conf. on Informatics in Control, Automation and Robotics), 2006*, Setúbal, 1, pp. 116-125.

Bastos Filho, T.F.; Ferreira, A.; Silva, R.L.; Celeste, W.C. & Sarcinelli Filho, M. (2007a). Human-Machine Interface Based on EMG and EEG Signals Applied to a Robotic Wheelchair. *Journal of Physics: Conference Series*, Vol. 90, ISSN 1742-6588.

Bastos Filho, T.F.; Ferreira, A.; Silva, R.L.; Celeste, W.C. & Sarcinelli Filho, M. (2007b). Human-Machine Interface Based on EMG and EEG Signals Applied to a Robotic Wheelchair. *Journal of Physics: Conference Series*, Vol. 90, ISSN 1742-6588.

Cover & Thomas. (2006). *Elements of Information Theory 2nd Ed.*, Wiley, 2006.

Farry, K. ; Walker, I. & Baraniuk, R.G. (1996). Myoelectric teleoperation of a complex robotic hand. *Proc. IEEE Int. Conf. Robotics and Automation*, pp. 775-788, ISBN :, conference location, month and year, publisher, city.

Ferreira, A. ; Auat Cheein F.A. ; Postigo J. ; Bastos Filho T.F. ; Carelli, R. & Sarcineli Filho M. (2006b). Teleoperação de um Manipulador para uma Cadeira de Rodas Usando Sinais de EEG IV Congresso Ibero-Americano Sobre Tecnologias de Apoio a Portadores de Deficiência. *Anais do IV Congresso Ibero-Americano Sobre Tecnologias de Apoio a Portadores de Deficiência*, 1, may 23-27, 2006.

Ferreira, A. ; Bastos Filho, T.F. ; Sarcinelli Filho, M. ; Auat Cheein, F.A. ; Postigo, J. & Carelli, R. (2006a). Teleoperation of an Industrial Manipulator Through a TCP/IP Channel Using EEG Signals. *Proc. of ISIE 2006, Int. Symp. on Industrial Electronics*, Montreal, vol. 1, pp. 3066–3071.

Ferreira, A.; Bastos Filho, T.F.; Sarcinelli Filho, M.; Auat Cheeín, F.; Postigo, J. & Carelli, R. (2006c). Teleoperation of an Industrial Manipulator Through a TCP/IP Channel Using EEG Signals. *Proc. Of the Int. Symposium on Industrial Electronics ISIE2006*, Montreal, 1, pp. 3066-3071.

Ferreira, A.; Celeste, W.C.; Auat Cheeín, F.; Bastos Filho, T.; Sarcinelli Filho, M. & Carelli, R. (2008). Human-machine interfaces based on EMG and EEG applied to robotic systems. Journal of NeuroEngineering and Rehabilitation, 5, 1-15.

Fishman, G.S. (1996). *Monte Carlo Concepts, Algorithms, and Applications*. New York, Springer-Verlag.

Fukuda, O. ; Tsuji, T. ; Kaneko, M. & Otsuka, A. (2003). A Human-Assisting Manipulator Teleoperated by EMG Signals and Arm Motions. *IEEE Trans. on Robotics and Automation*, 19, 210-222, ISSN: 1042-296X.

Kelly, R.; Carelli, R. & Soria, C. (2004). Sobre control cinemático de impedancia en robots industriales. *VI Congreso Mexicano de Robótica*, ISSN: 0035 0516, Torreón, México.

Lopez, N.M. ; di Sciascio, F.A. ; Soria, C.M. & Valentinuzzi M.E. (2009). Robust EMG sensing system based on data fusion for myoelectric control of a robotic arm. *BioMedical Engineering OnLine 2009*, pigs. 8:5. ISSN 1475-925X, doi:10.1186/1475-925X-8-5.

Lopez, N.M. ; Soria, C.M. ; Orosco, E.C. ; di Sciascio, F.A. & Valentinuzzi, M.E. (2007). Two-Dimensional Myoelectric Control of a Robotic Arm for Upper Limb Amputees. *Journal of Physics: Conference Series*, Vol. 90, ISSN 1742-6588.

Millan, J. ; Renkens, F. ; Mouriño, J. & Gerstne, W. (2004). Non-invasive brain-actuated control of a mobile robot. *Proc. of the 18th Int. Joint Conf. on Artificial Intelligence*, ISBN: 0-127-05661-0, Acapulco, Mexico.

Oskoei, M. & Hu, H. (2007). Myoelectric control systems. A survey. *Biomedical Signal Processing and Control*, Vol.2, pp. 275–294, ISSN: 1746-8094.

Papoulis, A. (1980). *Probabilidad, variables alatorias y procesos estocásticos*. Eunibar, Barcelona.

Sciavicco, L. & Siciliano, B. (2000). *Modelling and Control of Robot Manipulators 2nd Edition*, Advanced Textbooks in Control and Signal Processing Series. ISBN: 1852332212, Edited by Springer-Verlag, London, UK.

Wolpaw, J.R. ; Birbaumer, N. ; McFarland, D.J. ; Pfurtscheller, G. & Vaughan, T.M. (2002). Braincomputer interfaces for communication and control. *Clin. Neurophysiol,* Vol.113, Nº6, 767–791, ISSN: 1537-1603.

Yatsenko, D. ; McDonnall, D. & Guillory, S. (2007). Simultaneous, Proportional, Multi-axis Prosthesis Control using Multichannel Surface EMG. *Proc. 29th Annual Int. Conf. of the IEEE EMBS*, ISSN: 1557-170X, pp.6134-6141, August 23-26, 2007.

Zecca, M.; Micera, S.; Carrozza, M.C. & Dario, P. (2002). Control of Multifunctional Prosthetic Hands by Processing the Electromyographic Signal. *Critical Reviews in Biomedical Engineering*, Vol.30, pp.459-485, ISSN: 0278-940X.

Robot Manipulators New Achievements

Edited by Aleksandar Lazinica and Hiroyuki Kawai

ISBN 978-953-307-090-2
Hard cover, 718 pages
Publisher InTech
Published online 01, April, 2010
Published in print edition April, 2010

Robot manipulators are developing more in the direction of industrial robots than of human workers. Recently, the applications of robot manipulators are spreading their focus, for example Da Vinci as a medical robot, ASIMO as a humanoid robot and so on. There are many research topics within the field of robot manipulators, e.g. motion planning, cooperation with a human, and fusion with external sensors like vision, haptic and force, etc. Moreover, these include both technical problems in the industry and theoretical problems in the academic fields. This book is a collection of papers presenting the latest research issues from around the world.

How to reference

In order to correctly reference this scholarly work, feel free to copy and paste the following:

Fernando A. Auat Cheein, Fernando di Sciascio, Juan Marcos Toibero and Ricardo Carelli (2010). Robot Manipulator Probabilistic Workspace Applied to Robotic Assistance, Robot Manipulators New Achievements, Aleksandar Lazinica and Hiroyuki Kawai (Ed.), ISBN: 978-953-307-090-2, InTech, Available from: http://www.intechopen.com/books/robot-manipulators-new-achievements/robot-manipulator-probabilistic-workspace-applied-to-robotic-assistance

INTECH
open science | open minds

InTech Europe
University Campus STeP Ri
Slavka Krautzeka 83/A
51000 Rijeka, Croatia
Phone: +385 (51) 770 447
Fax: +385 (51) 686 166
www.intechopen.com

InTech China
Unit 405, Office Block, Hotel Equatorial Shanghai
No.65, Yan An Road (West), Shanghai, 200040, China
中国上海市延安西路65号上海国际贵都大饭店办公楼405单元
Phone: +86-21-62489820
Fax: +86-21-62489821

© 2010 The Author(s). Licensee IntechOpen. This chapter is distributed under the terms of the Creative Commons Attribution-NonCommercial-ShareAlike-3.0 License, which permits use, distribution and reproduction for non-commercial purposes, provided the original is properly cited and derivative works building on this content are distributed under the same license.

IntechOpen

IntechOpen